

A compatible finite element multi-material ALE hydrodynamics algorithm

A. J. Barlow^{*,†}

Design Physics Department, AWE Aldermaston, Berkshire RG74PR, U.K.

SUMMARY

The main ideas of compatible Lagrangian hydrodynamics were originally developed in the form of a finite volume scheme by Caramana *et al.* at LANL. A new compatible finite element Lagrangian hydrodynamics method has been developed and implemented in a 2D arbitrary Lagrangian Eulerian (ALE) code CORVUS. The new finite element method was developed in preference to the published finite volume schemes in order to see if the fundamental principles of compatible hydro could be translated across to other numerical methods in use in hydrocodes and to facilitate a more direct comparison of the performance of the compatible hydro scheme with the existing finite element scheme in CORVUS. The new finite element scheme provides total energy conservation to round off for the Lagrangian step. The edge artificial viscosities and sub-zonal pressures that have been introduced through the framework of the compatible hydro scheme provide further improvements in terms of accuracy and robustness for Lagrangian calculations. The details of the compatible finite element Lagrangian scheme and the extensions required to the scheme to allow it to be applied as the Lagrangian step of a multi-material ALE code are discussed. Test problems will be presented to demonstrate some of the benefits and the performance of the new method for hydrocode applications. © British Crown Copyright 2007/MOD. Reproduced with permission. Published by John Wiley & Sons, Ltd.

Received 27 April 2007; Revised 12 July 2007; Accepted 12 July 2007

KEY WORDS: ALE; Lagrangian; hydrodynamics; finite element methods; compressible flow; mesh adaption

1. INTRODUCTION

Arbitrary Lagrangian Eulerian (ALE) methods were first introduced in [1] to try and exploit the benefits of Lagrangian and Eulerian methods without suffering their deficiencies. These methods are usually implemented in hydrocodes by splitting each computational time step into a Lagrangian step and a rezone step. In order to fully exploit the benefits of this approach for many applications,

*Correspondence to: A. J. Barlow, Design Physics Department, AWE Aldermaston, Berkshire RG74PR, U.K.

†E-mail: andy.barlow@awe.co.uk

it is desirable to keep the mesh motion as Lagrangian as possible. Compatible Lagrangian hydrodynamics methods offer significant improvements in terms of accuracy and robustness over traditional Lagrangian schemes and so should also offer significant benefits if applied as the Lagrangian step of an ALE hydrocode.

In this paper a new compatible finite element Lagrangian hydrodynamics method has been developed and implemented in CORVUS, AWE's 2D ALE code. The new finite element method was developed in preference to the published finite volume compatible hydrodynamics schemes [3–6]; to see if the fundamental principles of compatible hydro could be translated across to other numerical methods in use in hydrocodes, to facilitate a more direct comparison of the performance of the compatible hydro scheme with the existing finite element scheme in CORVUS [7] and enabled rapid progress to be made as the existing physics in the code could be used immediately.

In order to apply the compatible hydro scheme as the Lagrangian step of a multi-material ALE code, a number of problems have had to be overcome. These include how to calculate the work done on individual material component within multi-material zones where the volume fraction may vary during the Lagrangian step, advect momentum given the new nodal mass definitions and advect the corner masses required by the compatible hydro scheme.

This paper will discuss the details of the compatible finite element Lagrangian scheme and the extensions required to apply the scheme as the Lagrangian step of a multi-material ALE code. Test problems will also be presented to demonstrate some of the benefits and the performance of the new method for hydrocode applications.

2. THE NUMERICAL METHOD

The compatible finite element ALE hydrodynamics method described here splits the computational time step into a Lagrangian step followed by a rezone step, which moves the grid and remaps the solution at the end of the Lagrangian step onto the new mesh.

2.1. Lagrangian step

Compatibility can simply be viewed as making the internal energy or work update consistent with the momentum update. This is achieved by replacing the usual PdV internal energy update by

$$M_z \frac{\partial e_z}{\partial t} = - \sum_p \mathbf{f}_p^z \cdot \mathbf{v}_p \quad (1)$$

where \mathbf{f}_p^z are the forces calculated during the momentum step for node p of zone z , M_z is the zone mass, e_z the specific internal energy of the zone and \mathbf{v}_p the velocity of the node.

In order to conserve total energy, the corner masses must also be treated as Lagrangian objects just like the zone masses. This ensures that there is no unaccounted for exchange of momentum between the nodes. The original CORVUS scheme defined the nodal mass in terms of an integral of the shape function associated with each node and so did not satisfy this property.

Compatible hydro has two main things to offer: total energy conservation to round off for the Lagrangian step without slide lines and an increased flexibility in the centring of forces that can be allowed within a zone. This allows sub-zonal pressures and edge-based forms of artificial viscosity to be included in a natural and consistent way. This in turn can be used to improve accuracy and robustness of a Lagrangian scheme.

Petrov Galerkin (or area weighting) has been retained when solving the momentum equation in cylindrical geometry to preserve spherical symmetry on axis. This leaves the finite element discretization of the force terms unchanged from what was described in [7].

However, in order to use these area weighted forces, the internal energy update (1) has to be modified as follows:

$$M_z \frac{\partial e_z}{\partial t} = - \sum_p r_p \mathbf{f}_p^z \cdot \mathbf{v}_p \quad (2)$$

where r_p is the radius of the node p . This is required to preserve symmetry in cylindrical geometry and to maintain total energy conservation.

2.1.1. Corner mass definition. In order for this form for the internal energy update to be valid, the corner masses must also be related to the area weighted corner masses in the same way as the area weighted forces used in the momentum step are related to the real forces.

$$(\rho A)_p = \frac{M_p}{r_p} \quad (3)$$

where ρ is the node density, A is the area associated with a node and M_p is the mass of the node. This means the finite element approach for defining the area weighted and real nodal masses used in the original CORVUS scheme [7] must be abandoned.

New area weighted corner masses can however be found by requiring the momentum equation to take the form:

$$M_p \frac{\partial \mathbf{v}_p}{\partial t} = r_p (\rho A)_p \frac{\partial \mathbf{v}_p}{\partial t} = r_p \sum_z \mathbf{f}_z^p \quad (4)$$

These areas can be calculated as suggested by Caramana *et al.* [3] by subdividing the zone into four triangles each with vertices given by the end points of a zone edge and the centre of the zone $r_c = (r_1 + r_2 + r_3 + r_4)/4$ and noting the true volume of each of these triangles is $A_i(r_i + r_{i+1} + r_c)/3$.

The volumes of these triangles will then sum to give the total volume of each zone. The expression obtained for the total cell volume can then be decomposed with respect to r_i to define the four new corner volumes. Simply dividing each corner volume by the radius of its vertex then gives the required area weights.

The corner masses corresponding to these volumes are calculated and stored at the start of the calculation. The volumes and areas are then recalculated every time step and the density required to match the corner mass with the new corner volume is used to define the area weighted masses used when solving the momentum equation.

Since the nodes on axis have zero mass as a consequence of (3), the area weighted corner masses are set for these nodes using the average cell density or the motion of the nodes is simply inferred from the nearest node off axis. In practice, it has been found that greater robustness is obtained by slaving the motion of the axial nodes. This is justified because the nodes on axis have no influence on the kinetic or internal energy within a simulation. This is because the axial nodes have no mass and because of the radial weighting in (2).

Two approaches have been found to be useful. The first simply calculates the nodal acceleration as discussed above, but if the node is detected to go outside its immediate neighbours, it is

repositioned to be at the centre of its two neighbours. The other approach that has been found to work well is to apply a velocity to the axial nodes that will preserve the current angle of the mesh line to the axis of symmetry.

2.1.2. Sub-zonal pressure scheme. The original numerical scheme in CORVUS used hourglass filters to remove non-physical hourglass modes. The new compatible hydro scheme has enabled a sub-zonal pressure scheme to be added which can be used as an alternative to the existing hourglass filters. Sub-zonal pressures potentially offer improved robustness in that they will act to suppress the collapse of the corner volumes. This can be effective against other numerical problems as well as hourglass modes, such as artificial vorticity, that may act over larger wavelengths and so cannot be suppressed by hourglass filters [5]. However, it is also possible that the sub-zonal pressures scheme could introduce stiffness into the numerical solution.

Corner masses are again required for the sub-zonal pressure scheme. But the corner masses discussed above in the context of solving the momentum equation are inappropriate as the masses and associated corner volumes are zero for nodes on axis. A new set of corner masses have been introduced for the sub-zonal pressure scheme by subdividing each element into four sub-elements defined by the four existing vertices, cell centre and four half-side points as shown in Figure 1.

The initial mass for these four volumes is stored for each cell and used each time step to define sub-zonal densities. The internal energy is assumed to be constant across the zone. Pressure perturbations relative to the average cell pressure are then estimated using the sound speed as follows:

$$\Delta p_{p,z} = c_{s,z}^2 \Delta \rho_{p,z} \quad (5)$$

where $c_{s,z}$ is the sound speed for the zone z , $\Delta p_{p,z}$ is the pressure perturbation and $\Delta \rho_{p,z}$ is the density difference between the corner volume and the average cell density. If the zone is a multi-material cell then a volume fraction weighted average of the material components sound speeds is used.

The sub-zonal pressures are then treated as perturbations to the element pressure and forces associated with these pressure perturbations are calculated using the normal finite element approach used in CORVUS but applied to each of the four subzones as shown in Figure 2.

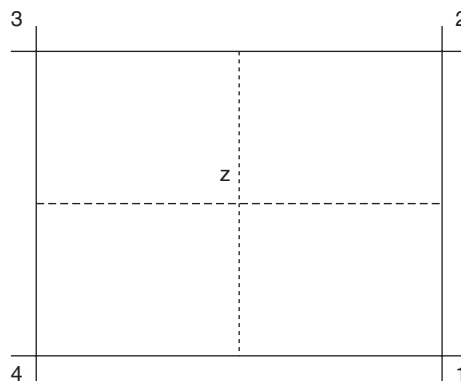


Figure 1. Sub-elements used to define sub-zonal pressures.

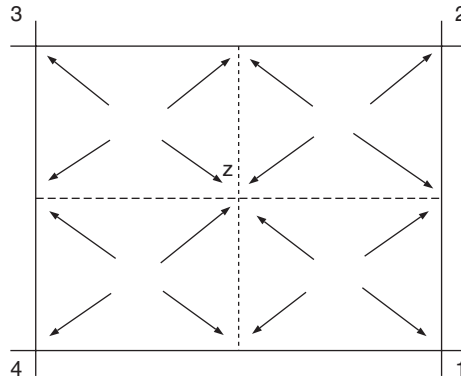


Figure 2. Forces calculated in sub-elements used to define sub-zonal pressures.

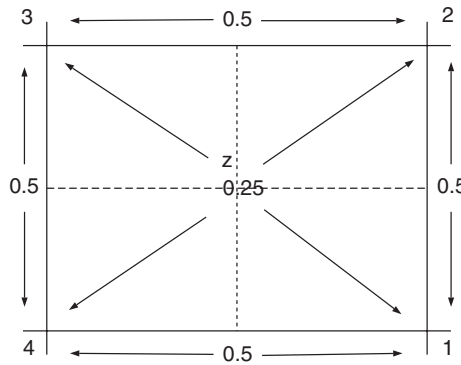


Figure 3. Distribution of forces calculated at non-dynamical points to dynamical points.

The centre point and half-side points are then treated as non-dynamical points with their associated forces being distributed to the appropriate dynamical points as shown in Figure 3. The subzone pressure perturbation forces are then added to the normal pressure forces for the zone. The nodal accelerations are then evaluated using these forces and the new nodal mass definitions.

2.1.3. Edge artificial viscosity. Compatible hydrodynamics enables edge-based artificial viscosities to be introduced. An edge-based artificial viscosity potentially offers improved robustness particularly for radiation hydrodynamics problems where large aspect ratio zones are often required. It also provides the opportunity to introduce a directional monotonic artificial viscosity that acts only in the direction normal to the shock front.

The monotonic edge-based artificial viscosity has been implemented largely following the method developed by Caramana *et al.* [4]. The force between local nodes 1 and 2 of element z , for example, due to the presence of an edge artificial viscosity is given by

$$\mathbf{f}_{21}^{\text{visc}} = c_1(1 - \psi_{21})\rho_z(c_{s,z} + \Delta v_{21})[\Delta \mathbf{v}_{21} \cdot \mathbf{S}_1]\Delta \hat{v}_{21} \tag{6}$$

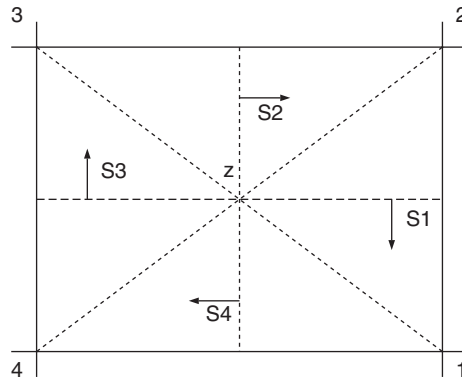


Figure 4. Notation for edge artificial viscosity.

where ρ_z is the density of the zone, $c_{s,z}$ the sound speed, c_1 a coefficient, $\Delta v_{21} = v_2 - v_1$ is the difference in velocity between local nodes 1 and 2 on edge 21; S_i is the median mesh vector associated with edge i , whose magnitude is equal to the area of the triangle defined by the centroid and the two nodes on the edge, whose direction is normal to the median mesh line as shown in Figure 4 and $[\Delta v_{21} \cdot S_1]$ is a compression switch. The compression switch returns a value of unity when the triangle associated with the edge is in compression and returns zero in expansion. An equal and opposite force is then applied to the two nodes defining the edge with the signs chosen to ensure the force resists compression and is hence dissipative. The form of the monotonic limiter ψ was as defined by Caramana in [4].

2.2. Extending compatible Lagrangian hydro into an ALE scheme

The key issues in applying a compatible Lagrangian hydrodynamics scheme as the Lagrangian step of a multi-material ALE method are how to advect the corner masses, perform momentum advection, perform the internal energy update for multi-material cells and move the mesh to exploit the benefits of the compatible Lagrangian hydrodynamics scheme.

2.2.1. Internal energy update for multi-material cells. Multi-material ALE introduces the need to handle mixed or multi-material cells that contain more than one material. A volume of fluid (VOF) scheme is used to represent these zones, where a volume fraction variable $F_{k,z}$ is used to describe the relative fraction of each cell occupied by each material and separate state variables are maintained for each material component.

In extending the compatible Lagrangian hydrodynamics scheme to multi-material ALE, the internal energy update (2) must be modified to provide a means of updating the internal energy of material components within multi-material cells in a consistent manner.

This is achieved by simply defining separate corner force components $f_{k,p}^z$ for each material k in multi-material cell z acting on node p . These force components are defined using the material components state variables, but integrated as though they are single material values. These multi-material force components are then used to update the internal energy of the multi-material cell

components as follows:

$$M_{k,z} \frac{\partial e_{k,z}}{\partial t} = - \sum_p r_p F_{k,z} \mathbf{f}_{k,p}^z \cdot \mathbf{v}_p \tag{7}$$

where $F_{k,z}$ is the volume fraction for the material component k in element z .

The internal energy update can also be made fully consistent with pressure relaxation schemes that allow the volume fractions to vary during the Lagrangian step as described in [7] by replacing the volume fraction in (7) with a relative compressibility factor.

2.2.2. Mesh movement. In order to fully exploit the benefits of the compatible hydrodynamics scheme, it is desirable that the mesh motion is kept as close to Lagrangian as possible, while still retaining robustness for high material deformation. A local mesh movement strategy has been developed to achieve this, which has been motivated by corner volumes used in the compatible hydro scheme. This local mesh movement strategy simply defines whether a node should be allowed to relax or not. If the relaxation criterion is not reached, the node is restricted to remain Lagrangian. If it is satisfied then a user defined mesh movement algorithm is applied. In most cases this is based on Winslow’s equipotential mesh relaxation algorithm [2].

There are two main criteria that are applied. The first of which senses the collapse of a corner area relative to the total cell area and the second detects corner angles that are collapsing. The first criterion is expressed in area rather than volume to preserve symmetry for cylindrical geometry. As it is normally desirable to keep resolution in regions of high importance material interface nodes are treated differently from internal nodes making such nodes less likely to relax. Interface nodes are defined as the nodes on cell edges that are adjacent to different materials in order to also capture material interfaces represented by multi-material cells.

Once an internal node meets the relaxation criterion, it is allowed to relax for the rest of the simulation. While interface nodes must satisfy the relaxation criterion each time step.

The area criterion for mesh relaxation of internal nodes is expressed as

$$\frac{4ca_{k,z}}{A_z} < a_r \tag{8}$$

where $ca_{k,z}$ is the corner area for element z and local node k , A_z is the element area and a_r is a user defined relative area which must be less than or equal to unity and is typically about 0.5.

The angle criterion for mesh relaxation of internal nodes is expressed as

$$\text{Sin}(\theta) < t_r \tag{9}$$

where θ is the corner angle and t_r is a user defined value which is typically about 0.87.

At material interface nodes both criteria are applied. However, for the area criterion to trigger relaxation it must be met at least once in each of the materials associated with the node. This approach was not taken with the relative angle test as it is common to have far more shear on one side of a material interface than the other due to differences in shock speed or material strength. Initial zoning that would immediately trigger relaxation can also be preserved by modifying the criterion for relaxation given above to include weights based on the initial area ratios and angles.

2.2.3. Advection of corner masses. The compatible finite element Lagrangian scheme requires two types of corner mass, one that is used in solving the momentum equation and the other which

is used to calculate the sub-zonal pressures used to remove hourglass modes. In extending this scheme into a full multi-material ALE method, both types of corner mass must be updated within each zone when the mesh is moved during the rezone step to account for the fluxes of material entering and leaving each cell.

Since an advection scheme is used in CORVUS to define the new element and node-centred variables, the corner masses can be updated by noting that the new element mass post advection can be expressed as

$$M_z^{\text{new}} = M_z^{\text{old}} - \sum_{k=1}^4 \Delta m_{z,k}^{\text{out}} + \sum_{k=1}^4 \Delta m_{z,k}^{\text{in}} \quad (10)$$

where M_z^{old} is the element mass at the end of the Lagrangian step, $\sum_{k=1}^4 \Delta m_{z,k}^{\text{out}}$ is the mass flux leaving the zone and $\sum_{k=1}^4 \Delta m_{z,k}^{\text{in}}$ is the mass flux entering the zone.

Both types of corner mass can then be updated as follows:

$$cm_{z,k}^{\text{new}} = \frac{cm_{z,k}^{\text{old}}}{M_z^{\text{old}}} \left(M_z^{\text{old}} - \sum_{k=1}^4 \Delta m_{z,k}^{\text{out}} \right) + \frac{cv_{z,k}^{\text{new}}}{V_z^{\text{new}}} \sum_{k=1}^4 \Delta m_{z,k}^{\text{in}} \quad (11)$$

where $cm_{z,k}^{\text{old}}$ is the corner mass for element z and local node k at the end of the Lagrangian step, $cv_{z,k}^{\text{new}}$ is the new post remap corner volume and V_z^{new} is the new post remap element volume.

This ensures that any mass remaining in the cell after advection is distributed to the corners in the same proportions as the original cell mass was prior to advection. This is very important as it ensures the limiting case of Lagrangian mesh motion is satisfied. Any new mass entering the cell during the advection step is distributed in proportion to the corner volumes. This assumes that new mass entering the cell during the advection step comes in at constant density. This again satisfies the other important limit that if all the mass present in the zone at the end of the Lagrangian step is fluxed out, then the sub-zonal pressures will be uniform throughout the element so there will be no artificial forces introduced to suppress hourglass modes.

2.2.4. Momentum advection. A choice must also be made of what nodal mass to use when advecting momentum. The most natural choice would be to construct the nodal mass from the corner masses used in the Lagrangian step to solve the momentum equation. However, this would result in zero mass nodes on axis, which could not be advected in a consistent manner. In order to overcome this problem the nodal mass at the end of the Lagrangian step used for the momentum advection was taken as the sum of the corner masses used for calculating sub-zonal pressures of the adjacent elements sharing the node in question. This avoids the problem of zero mass nodes on axis, while retaining some influence of the corner masses and so should be less diffusive and improve the total energy conservation of the ALE scheme.

Currently the nodal mass flux is obtained by taking an average of the element mass fluxes for the same logical edge of the four elements adjacent to the node. However, a more consistent approach which may improve kinetic energy conservation would be to also use the form of (11) to define the nodal mass fluxes required for the momentum advection.

3. NUMERICAL RESULTS

Results from two well-known hydrocode test problems will now be presented to illustrate some of the benefits of the new scheme. Results obtained using the pure Lagrangian scheme will be presented to allow direct comparisons to be made with the results published in [3–6]. Further results will be presented in a future paper for the multi-material ALE simulations.

3.1. Noh's problem

Noh's problem is a well-known test of artificial viscosity methods. It consists of a single region of ideal gas with ratio of specific heats $\gamma = 1.66$, zero initial internal energy, unity initial density and a unity radial initial velocity distribution acting towards the origin. It can be calculated in plane, cylindrical or spherical geometry, but only the more testing spherical geometry problem will be considered here. The initial mesh used for Noh's problem was chosen to match that used in [4].

The mesh at $0.6 \mu\text{s}$ is shown in Figure 5. The analytic solution for density behind shock for the spherical problem at $0.6 \mu\text{s}$ is 64.0 g/cc . Density profiles are given in Figure 6 for three simulations calculated with: the original CORVUS PdV scheme with an element-centred artificial viscosity and hourglass filter, original CORVUS hydro scheme with an energy fix added for the work done by the hourglass filter and compatible hydro with edge artificial viscosity and sub-zonal pressure scheme. The compatible hydro with edge q gives a result close to analytic solution and shows a small improvement over scalar monotonic viscosity. The original PdV hydro scheme in CORVUS overshoots the analytical solution unless energy correction is included for work done by hourglass filter.

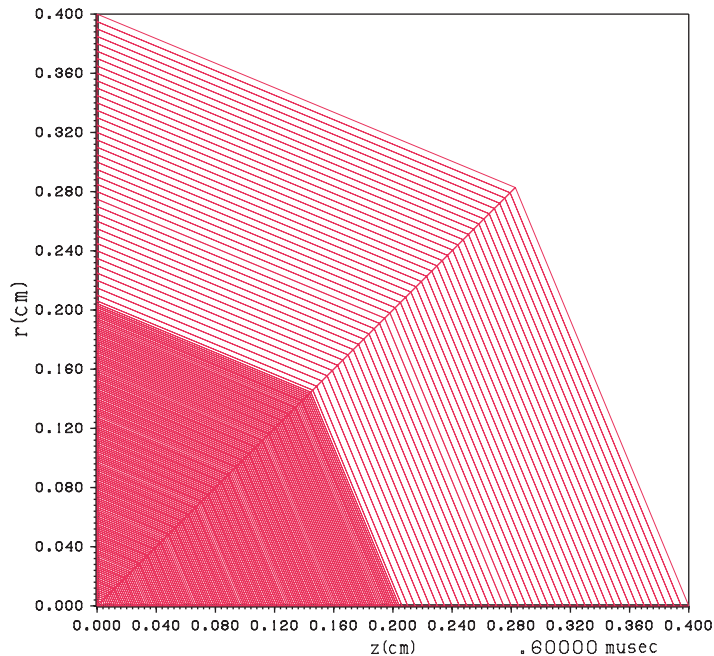


Figure 5. Mesh for the Noh problem at $0.6 \mu\text{s}$.

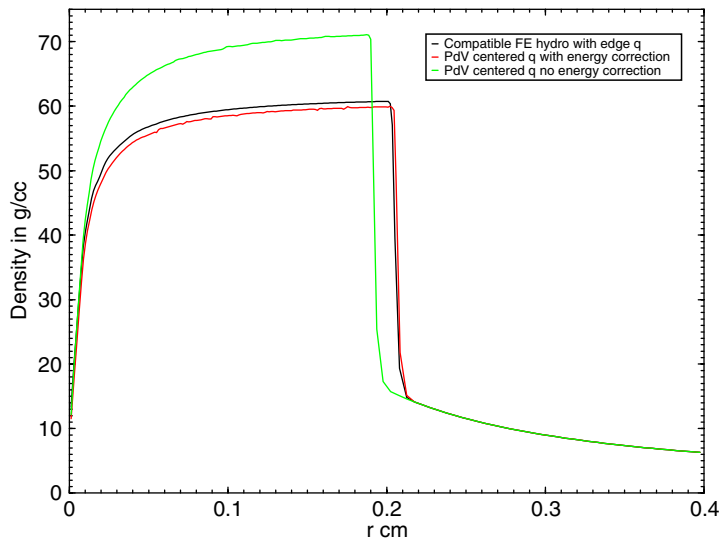


Figure 6. Density profiles for the Noh problem at $0.6 \mu\text{s}$.

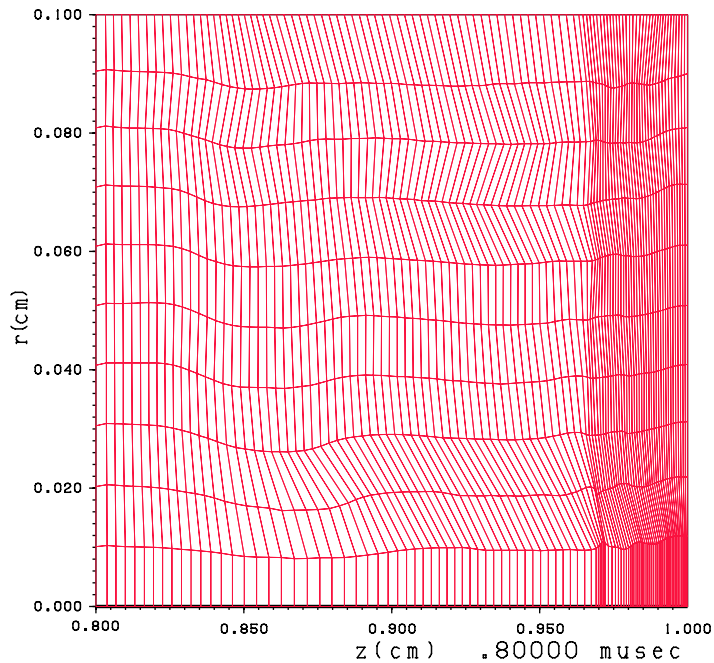


Figure 7. Mesh for Saltzman's piston problem at $0.8 \mu\text{s}$ calculated with compatible hydro with edge artificial viscosity.

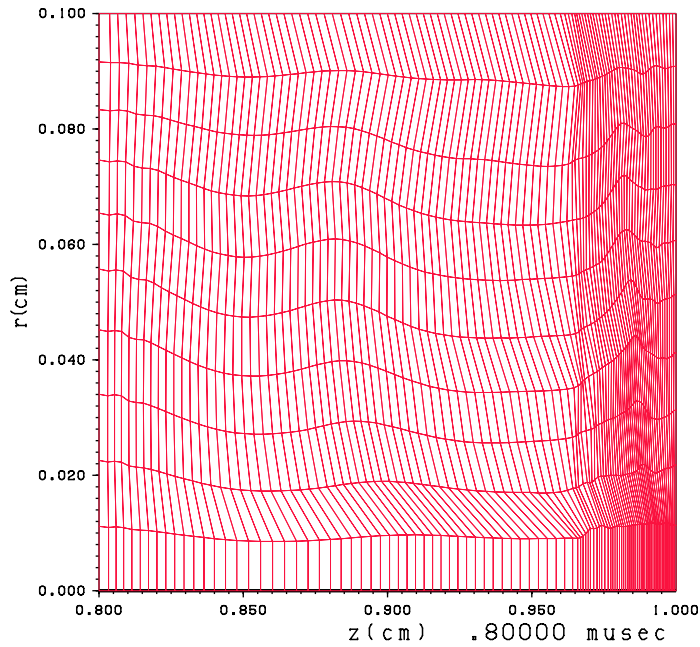


Figure 8. Mesh for Saltzman's piston problem at $0.8\mu s$ calculated with compatible hydro with edge artificial viscosity and sub-zonal pressures.

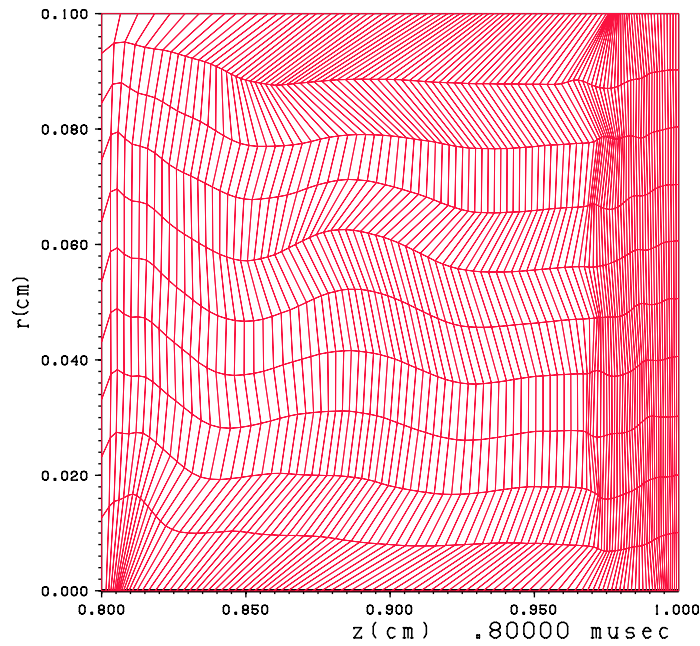


Figure 9. Mesh for Saltzman's piston problem at $0.8\mu s$ calculated with PdV hydro with element centred artificial viscosity and hourglass filter.

3.2. Saltzman's piston

Saltzman's piston problem consists of a cylinder of gas with a piston moving with a velocity of unity at one end and a reflecting boundary at the other. An ideal gas equation of state is assumed with ratio of specific heats $\gamma = 1.66$, zero initial internal energy and unity initial density. The initial mesh is skewed from the vertical with a half sin wave perturbation as described in [5]. Results at $0.8 \mu\text{s}$ are presented to enable comparison with the solutions presented in [5].

A good solution was obtained with the compatible finite element Lagrangian hydrodynamics scheme with the edge artificial viscosity alone as shown in Figure 7.

The solution obtained with compatible finite element hydro scheme is further improved by also using the sub-zonal pressure scheme in addition to the edge artificial viscosity as shown in Figure 8.

The solution obtained with the new compatible finite element hydro scheme offers a significant improvement over the results obtained with the original PdV-based scheme in CORVUS with an element centred monotonic artificial viscosity and an hourglass filter which are shown in Figure 9.

4. CONCLUSIONS

A new compatible finite element ALE hydro scheme has been developed and implemented in the 2D ALE hydrocode CORVUS. This has demonstrated that the main ideas of compatible finite volume hydrodynamics can be transferred across to finite element methods. A method has also been proposed for extending the compatible Lagrangian hydrodynamics method into a compatible multi-material ALE hydrodynamics method. Two test problems have also been presented which illustrate the benefits of the new method.

REFERENCES

1. Hirt CW, Amsden AA, Cook JL. An arbitrary Lagrangian–Eulerian computing method for all flow speeds. *Journal of Computational Physics* 1974; **14**:227–253.
2. Winslow AM. Numerical solution of the quasilinear Poisson computing equation in a nonuniform triangular mesh. *Journal of Computational Physics* 1967; **2**:149–172.
3. Caramana EJ, Burton DE, Shashkov MJ, Whalen PP. The construction of compatible hydrodynamics algorithms utilizing conservation of total energy. *Journal of Computational Physics* 1998; **146**:227–262.
4. Caramana EJ, Shashkov MJ, Whalen PP. Formulations of artificial viscosity for multi-dimensional shock wave computations. *Journal of Computational Physics* 1998; **144**:70–97.
5. Caramana EJ, Shashkov MJ. Elimination of artificial grid distortion and hourglass-type motions by means of Lagrangian sub-zonal masses and pressures. *Journal of Computational Physics* 1998; **142**:521–561.
6. Caramana EJ, Whalen PP. Numerical preservation of symmetry properties of continuum problems. *Journal of Computational Physics* 1998; **141**:174–198.
7. Barlow AJ. Multi-material arbitrary Lagrangian–Eulerian algorithm for computational shock hydrodynamics. *Ph.D. Thesis*, University of Wales, Swansea, 2002.